Steel and Composite Structures, *Vol. 36, No. 3 (2020) 355-367*
DOI: https://doi.org/10.12989/scs.2020.36.3.355

A four-unknown refined plate theory for dynamic analysis of FG-sandwich plates under various boundary conditions

Abderrahmane Menasria[1,2], Abdelhakim Kaci*[1,3], Abdelmoumen Anis Bousahla[4,5], Fouad Bourada[1,5,6], Abdeldjebbar Tounsi[1,5], Kouider Halim Benrahou[1,5], Abdelouahed Tounsi[1,5], E.A. Adda Bedia[5] and S.R. Mahmoud[7]

[1]*Material and Hydrology Laboratory, University of Sidi Bel Abbes, Faculty of Technology, Civil Engineering Department, Algeria*
[2]*Université de Abbés Laghrour Khenchela, Faculté de Sciences & Technologie, Département de Génie Civil, Algeria*
[3]*Université Dr Tahar Moulay, Faculté de Technologie, Département de Génie Civil et Hydraulique, BP 138 Cité En-Nasr 20000 Saida, Algérie*
[4]*Laboratoire de Modélisation et Simulation Multi-échelle, Département de Physique, Faculté des Sciences Exactes, Département de Physique, Université de Sidi Bel Abbés, Algeria*
[5]*Department of Civil and Environmental Engineering, King Fahd University of Petroleum & Minerals, 31261 Dhahran, Eastern Province, Saudi Arabia*
[6]*Département des Sciences et de la Technologie, centre universitaire de Tissemsilt, BP 38004 Ben Hamouda, Algérie*
[7]*GRC Department, Jeddah Community College, King Abdulaziz University, Jeddah, Saudi Arabia*

(*Received May 13, 2019, Revised July 10, 2020, Accepted July 13, 2020*)

Abstract. The current work, present dynamic analysis of the FG-sandwich plate seated on elastic foundation with various kinds of support using refined shear deformation theory. The present analytical model is simplified which the unknowns number are reduced. The zero-shear stresses at the free surfaces of the FG-sandwich plate are ensured without introducing any correction factors. The four equations of motion are determined via Hamilton's principle and solved by Galerkin's approach for FG-sandwich plate with three kinds of the support. The proposed analytical model is verified by comparing the results with those obtained by other theories existing in the literature. The parametric studies are presented to detect the various parameters influencing the fundamental frequencies of the symmetric and non-symmetric FG-sandwich plate with various boundary conditions.

Keywords: dynamic analysis, FG-sandwich plates; RPT model; Galerkin's approach and various boundary conditions

1. Introduction

In the recent years, the studies research on the sandwich structures has increased sharply because of their advantages such as (excellent ratio stiffness/mass, a good ability to absorb the energy and high shock wave resistant). These studies can be found in the works of (Pagani *et al.* 2016, Tornabene *et al.* 2017, Kolahchi 2017, Rekatsinas and Saravanos 2017, Szekrényes 2018, Chen *et al.* 2018, Tornabene and Brischetto 2018, Badriev *et al.* 2018, Moradi-Dastjerdi and Behdinan 2019, Mehar *et al*. 2019). Several theories and models have been developed which can be useful to analyze the behaviors of sandwich structures. Thai *et al*. (2015) developed a novel numerical approach based on TSDT and isogeometric approach for studying bending, buckling and free vibrational behaviors of laminated composite plate. Tan *et al.* (2017) analyzed static and dynamic behaviors of FG plate by employing the XIGA based on the Bézier extraction and two-variable RPT. A three-dimensional (3D) IGA-meshfree coupling approach is presented by Tan *et al*. (2018) to examine Static, dynamic and buckling of FG plates and shells. After the development of the new range of advanced materials (FGM), the FG-sandwich plates are classified as an exceptional efficient type of sandwich structure. These specific classes of structures (FG-sandwich plates) are widely investigated by several scientists' researchers. Iurlaro *et al.* (2014) developed a refined zigzag theory (RZT) for static and dynamic analysis of the simply supported and clamped FG-sandwich plate subjected to bi-sinusoidal and uniform loads. Duc *et al*. (2015) studied the dynamic analysis of imperfect eccentrically stiffened shear deformable sandwich plate in thermal environment. Using HSDT model Dinh Duc and Hong Cong (2016) analyzed Nonlinear thermo-mechanical dynamic response of piezoelectric FG- sandwich plates on elastic foundations. The mechanical analysis of FG sandwich plates on elastic foundation is examined by Akavci (2016) using a new hyperbolic shear and normal deformation plate theory. Do *et al*. (2017) examined the material combination role on mechanical response of FG sandwich plates in thermal environment. The Flexural dynamic analysis of FG-sandwich plates resting on elastic foundation with various boundary conditions is examined by Tossapanon and Wattanasakulpong (2017) employing the Chebyshev collocation technique. Based on higher-order layerwise FE formulation, Pandey and Pradyumna (2018) studied a static and dynamic response of the FG-sandwich plate with two configurations of the sandwich Layers. Moita *et al.* (2018) have used a simple finite

∗Corresponding author, Professor
E-mail: kaci_abdelhakim@yahoo.fr

http://www.techno-press.org/?journal=scs&subpage=8
ISSN: 1229-9367 (Print), 1598-6233 (Online)

element model to examine a dynamic response of multilayer sandwich plates/shells with a viscoelastic core.based on the Hoff assumptions, Li *et al.* (2018) developed a new model for the static analysis of sandwich plates with FG-soft core. also other theories and models have been developed over the last two years to analyze the various behaviors of the FG-sandwich structures such as (Yoosefian *et al.* 2019, Hosseini *et al.*2019, Khorshidi and Karimi 2019, Gholamzadeh babaki and Shakouri 2019, Liu *et al.* 2019, Mirzaalian *et al.* 2019, Rezaiee-Pajand *et al.* 2019, Zouatnia and Hadji 2019, Li 2020a, b, Dorduncu 2020)

Through the literature it appears that it is necessary to study the FG sandwich structures behaviors with the different types of edges supports, for this purpose, the aim of the current work is to develop a four variables hyperbolic-exponential refined theory for dynamic analysis of the FG-sandwich plate resting on Winkler–Pasternak elastic foundation with various boundary conditions. Equations of motion are derived using Hamilton's principle and resolved via Galerkin's approach, The accuracy of the present theoretical model is verified by comparing the solution of FG sandwich plate with various others studies. The influences of the the power-law exponent, foundation parameters, geometry, aspect and layer thickness ratios on the frequency response of clamped and simply supported FG sandwich are deeply discussed.

2. Mathematical formulation

2.1 The FG sandwich plates properties

In this work the FG sandwich structure is composed from three isotropic layers and is assumed to be reposed on a Winkler–Pasternak type elastic foundation with the Winkler stiffness of k_w and shear stiffness of k_s as shown in Fig. 1.

The FG-sandwich plate has length a , width b and thickness *h*. the plate is supported at all four edges defined in the coordinate system (*x, y, z*) with x- and y-axes located in the middle plane ($z=0$) and its origin placed at the corner of the plate. The location of the x- and y-axes are in $z=0$ (the middle plane) and its origin placed at the corner of the plate. The lower and upper interfaces of the core are denoted h_1 and h_2 , respectively.

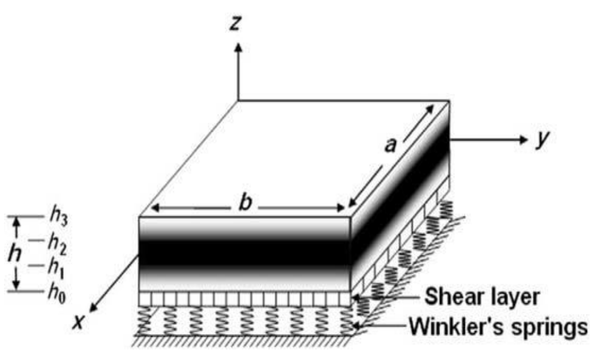

Fig. 1 Geometry of the FGM sandwich plate resting on elastic foundations

The bottom FG-skin varies from a metal-rich surface $(z=h_0=-h/2)$ to a ceramic-rich surface (h_1) while the top FG-skin face varies from a ceramic-rich surface (h_2) to a metal-rich surface $(z=h_3=h/2)$. The isotropic core situated between the two skins cited is totally ceramic.

In this work the FG- face sheets materials properties are assumed to vary according to a continuous power law function (Lal *et al.* 2017, Rezaiee-Pajand *et al.* 2018, Sahouane *et al*. 2019)

$$P(z)=\left(P_c-P_m\right)V(z)^{(n)}+P_m, \qquad (n=1,2,3) \tag{1}$$

where subscripts *c* and *m* indicate the ceramic and metal, respectively, *P* represent the effective material characteristic such as mass density *ρ(z),* Young's modulus E(z) and Poisson's ratio $\nu(z)$ and $V(z)^{(n)}$ is the volume fraction of the ceramic phase of each layer (n) is obtained from a simple rule of mixtures as

$$\begin{aligned} &V^{(1)}=\left(\frac{z-h_0}{h_1-h_0}\right)^p, && z\in[h_0,h_1] \\ &V^{(2)}=1, && z\in[h_1,h_2] \\ &V^{(3)}=\left(\frac{z-h_3}{h_2-h_3}\right)^p, && z\in[h_2,h_3] \end{aligned} \tag{2}$$

Where p represent the volume fraction index with $(p\ge 0)$, The metal volume fraction is given as $V_m=1-V_c$.

2.2. Constitutive equations

In the current investigation, for elastic and isotropic FGMs, the constitutive relations (stress-strain) can be written as:

$$\begin{aligned} \begin{Bmatrix}\sigma_x\\ \sigma_y\\ \tau_{xy}\end{Bmatrix}^{(n)} &= \begin{bmatrix}Q_{11} & Q_{12} & 0\\ Q_{12} & Q_{22} & 0\\ 0 & 0 & Q_{66}\end{bmatrix}^{(n)} \begin{Bmatrix}\varepsilon_x\\ \varepsilon_y\\ \gamma_{xy}\end{Bmatrix}^{(n)} \\ \begin{Bmatrix}\tau_{yz}\\ \tau_{xz}\end{Bmatrix}^{(n)} &= \begin{bmatrix}Q_{44} & 0\\ 0 & Q_{55}\end{bmatrix}^{(n)} \begin{Bmatrix}\gamma_{yz}\\ \gamma_{xz}\end{Bmatrix}^{(n)} \end{aligned} \tag{3}$$

where (σ and τ) and (ε and γ) are the stress and strain components, respectively. Q_{ij} are the stiffness coefficients expressed by

$$Q_{11}^{(n)}=Q_{22}^{(n)}=\frac{E^{(n)}(z)}{1-\nu^2}, \tag{4a}$$

$$Q_{12}^{(n)}=\frac{\nu E^{(n)}(z)}{1-\nu^2}, \tag{4b}$$

$$Q_{44}^{(n)}=Q_{55}^{(n)}=Q_{66}^{(n)}=\frac{E^{(n)}(z)}{2(1+\nu)}, \tag{4c}$$

In this work, the conventional HSDT assumptions are used and simplified to reduce the number of unknown variables. The displacement field functions of the classical

HSDT are given as

$$\begin{aligned} u(x,y,z,t) &= u_0(x,y,t) - z\frac{\partial w_0}{\partial x} + f(z)\phi_x(x,y,t) \\ v(x,y,z,t) &= v_0(x,y,t) - z\frac{\partial w_0}{\partial y} + f(z)\phi_y(x,y,t) \\ w(x,y,z) &= w_0(x,y,t) \end{aligned} \tag{5}$$

Where f(z) is the warping function and the terms u_0, v_0, w_0, ϕ_x, ϕ_y are the five unknown displacement of the mid-plane of the sandwich FG-plate.

Based on the conventional higher shear deformation model and dividing the deflection to bending and shear components $(w(x,y,z,t) = w_b(x,y,t) + w_s(x,y,t))$. The current displacement fields mentioned above can be written as follows

$$\begin{aligned} u(x,y,z,t) &= u_0(x,y,t) - z\frac{\partial w_b}{\partial x} - \left(z - h\sin\left(\frac{z}{h}\right) e^{-2\left(\frac{z}{h}\right)^2} \right)\frac{\partial w_s}{\partial x} \\ v(x,y,z,t) &= v_0(x,y,t) - z\frac{\partial w_b}{\partial y} - \left(z - h\sin\left(\frac{z}{h}\right) e^{-2\left(\frac{z}{h}\right)^2} \right)\frac{\partial w_s}{\partial y} \\ w(x,y,z,t) &= w_b(x,y,t) + w_s(x,y,t) \end{aligned} \tag{6}$$

The zero transverse shear stresses are ensured on the free surfaces of the FG sandwich plate (top and bottom surfaces) without introducing the shear correction factors.

Based on the current displacement field of Eq. (6). The nonzero linear strain components are obtained as

$$\begin{Bmatrix} \varepsilon_x \\ \varepsilon_y \\ \gamma_{xy} \end{Bmatrix} = \begin{Bmatrix} \varepsilon_x^0 \\ \varepsilon_y^0 \\ \gamma_{xy}^0 \end{Bmatrix} + z\begin{Bmatrix} k_x^b \\ k_y^b \\ k_{xy}^b \end{Bmatrix} + f(z)\begin{Bmatrix} k_x^s \\ k_y^s \\ k_{xy}^s \end{Bmatrix}, \quad \begin{Bmatrix} \gamma_{yz} \\ \gamma_{xz} \end{Bmatrix} = g(z)\begin{Bmatrix} \gamma_{yz}^0 \\ \gamma_{xz}^0 \end{Bmatrix} \tag{7}$$

$$g(z) = z - \left(\cosh(z) e^{-2z^2} - 4\sinh(z) z e^{-2z^2} \right) \tag{8}$$

where

$$\begin{Bmatrix} \varepsilon_x^0 \\ \varepsilon_y^0 \\ \gamma_{xy}^0 \end{Bmatrix} = \begin{Bmatrix} \dfrac{\partial u_0}{\partial x} \\ \dfrac{\partial v_0}{\partial y} \\ \dfrac{\partial u_0}{\partial y} + \dfrac{\partial v_0}{\partial x} \end{Bmatrix}, \quad \begin{Bmatrix} k_x^b \\ k_y^b \\ k_{xy}^b \end{Bmatrix} = \begin{Bmatrix} -\dfrac{\partial^2 w_b}{\partial x^2} \\ -\dfrac{\partial^2 w_b}{\partial y^2} \\ -2\dfrac{\partial^2 w_b}{\partial x \partial y} \end{Bmatrix},$$

$$\begin{Bmatrix} k_x^b \\ k_y^b \\ k_{xy}^b \end{Bmatrix} = \begin{Bmatrix} -\dfrac{\partial^2 w_s}{\partial x^2} \\ -\dfrac{\partial^2 w_s}{\partial y^2} \\ -2\dfrac{\partial^2 w_s}{\partial x \partial y} \end{Bmatrix}, \quad \begin{Bmatrix} \gamma_{yz}^0 \\ \gamma_{xz}^0 \end{Bmatrix} = \begin{Bmatrix} \dfrac{\partial w_s}{\partial y} \\ \dfrac{\partial w_s}{\partial x} \end{Bmatrix} \tag{9}$$

2.3 Equations of motion

The equations of motion compatible on the displacement field of Eq. (6) and deformations of Eq. (7) are derived from the Hamilton's principle given as (Abdelmalek *et al.* 2017, Safa *et al.* 2019)

$$0 = \int_0^t \left(\delta U + \delta U_{EF} + \delta K \right) dt \tag{10}$$

where δU is the strain energy variation, δU_F is the additional strain energy given by the elastic foundations, and δK is the kinetic energy. The first variation of strain energy of the current model can be written as

$$\begin{aligned} \delta U &= \int_A \int_{-h/2}^{h/2} \left(\sigma_x^{(n)} \delta\varepsilon_x + \sigma_y^{(n)} \delta\varepsilon_y + \tau_{xy}^{(n)} \delta\gamma_{xy} + \tau_{xz}^{(n)} \delta\gamma_{xz} + \tau_{yz}^{(n)} \delta\gamma_{yz} \right) dA dz \\ &= \int_A \left[N_x \delta\, \varepsilon_x^0 + N_{xy} \delta\gamma_{xy}^0 + N_y \delta\, \varepsilon_y^0 + M_x^b \delta\, k_x^b + M_y^b \delta\, k_y^b + M_{xy}^b \delta\, k_{xy}^b \right. \\ &\quad \left. + M_x^s \delta\, k_x^s + M_y^s \delta\, k_y^s + M_{xy}^s \delta\, k_{xy}^s + Q_{yz} \delta\gamma_{yz}^0 + Q_{xz} \delta\gamma_{xz}^0 \right] dA \end{aligned} \tag{11}$$

where A is the top surface. N, M *and* Q are stresses and moments resultants of the FG sandwich plate.

By integrating Eq. (3) over the thickness, the stresses and moments resultants N, M *and* Q are written as

$$\begin{Bmatrix} N_{xx}, & N_{yy}, & N_{xy} \\ M_{xx}^b, & M_{yy}^b, & M_{xy}^b \\ M_{xx}^b, & M_{yy}^b, & M_{xy}^b \end{Bmatrix} = \sum_{n=1}^{3} \int_{h_{n-1}}^{h_n} \left(\sigma_x, \sigma_y, \tau_{xy} \right)^{(n)} \begin{Bmatrix} 1 \\ z \\ f(z) \end{Bmatrix} dz, \tag{12a}$$

$$\left(Q_{xz}, Q_{yz} \right) = \sum_{n=1}^{3} \int_{h_{n-1}}^{h_n} \left(\tau_{xz}, \tau_{yz} \right)^{(n)} g(z) dz. \tag{12b}$$

where h_n and h_{n-1} are the top and bottom z-coordinates of the nth layer.

The expression of the strain energy induced by elastic foundations can be given as

$$\delta U_{EF} = \int_A f_e \delta w dA \tag{13}$$

where f_e is the reaction force of elastic foundation and can be expressed as

$$f_e = k_w w - k_{sx} \frac{\partial^2 w}{\partial x^2} - k_{sy} \frac{\partial^2 w}{\partial y^2} \tag{14}$$

where the parameters k_w and (k_{sx} and k_{sy}) are the Winkler and Pasternak modulus of subgrade reaction. If the shear layer foundation stiffness is neglected $(k_{sx} = k_{sy} = k_s = 0)$, Pasternak foundation becomes a Winkler foundation. If foundation is isotropic and homogeneous, we will get $k_{sx} = k_{sy} = k_s$.

The variation of kinetic energy δK is expressed as

$$\delta K = \int_V (\dot{u}\,\delta\dot{u} + \dot{v}\,\delta\dot{v} + \dot{w}\delta\dot{w})\rho(z)dV$$
$$= \int_A \{ I_0\left[\dot{u}_0\delta\dot{u}_0 + \dot{v}_0\delta\dot{v}_0 + \left(\dot{w}_b + \dot{w}_s\right)\delta\left(\dot{w}_b + \dot{w}_s\right)\right]$$
$$-I_1\left(\dot{u}_0\frac{\partial\delta\dot{w}_b}{\partial x} + \frac{\partial\dot{w}_b}{\partial x}\delta\dot{u}_0 + \dot{v}_0\frac{\partial\delta\dot{w}_b}{\partial y} + \frac{\partial\dot{w}_b}{\partial y}\delta\dot{v}_0\right)$$
$$+I_2\left(\frac{\partial\dot{w}_b}{\partial x}\frac{\partial\delta\dot{w}_b}{\partial x} + \frac{\partial\dot{w}_b}{\partial y}\frac{\partial\delta\dot{w}_b}{\partial y}\right) \tag{15}$$
$$-J_1\left(\dot{u}_0\frac{\partial\delta\dot{w}_s}{\partial x} + \frac{\partial\dot{w}_s}{\partial x}\delta\dot{u}_0 + \dot{v}_0\frac{\partial\delta\dot{w}_s}{\partial y} + \frac{\partial\dot{w}_s}{\partial y}\delta\dot{v}_0\right)$$
$$+K_2\left(\frac{\partial\dot{w}_s}{\partial x}\frac{\partial\delta\dot{w}_s}{\partial x} + \frac{\partial\dot{w}_s}{\partial y}\frac{\partial\delta\dot{w}_s}{\partial y}\right)$$
$$+J_2\left(\frac{\partial\dot{w}_b}{\partial x}\frac{\partial\delta\dot{w}_s}{\partial x} + \frac{\partial\dot{w}_s}{\partial x}\frac{\partial\delta\dot{w}_b}{\partial x} + \frac{\partial\dot{w}_b}{\partial y}\frac{\partial\delta\dot{w}_s}{\partial y} + \frac{\partial\dot{w}_s}{\partial y}\frac{\partial\delta\dot{w}_b}{\partial y}\right)\}\,dA,$$

where $\rho(z)$ is the mass density, the dot-superscript convention represent the differentiation with respect to the time variable t, the terms $(I_0, I_1, I_2, J_1, J_2, K_2)$ are the mass inertias defined as

$$(I_0, I_1, I_2) = \int_{-h/2}^{h/2} \left(1, z, z^2\right)\rho(z)dz \tag{16a}$$

$$(J_1, J_2, K_2) = \int_{-h/2}^{h/2} \left(f(z), z\,f(z), f^2(z)\right)\rho(z)dz \tag{16b}$$

By Substituting the Eqs. (11), (13) and (15) into Eq. (10), integrating by parts, separating and collecting the coefficients of displacements δu_0, δv_0, δw_b and δw_s, the equations of motion of the FG sandwich plate are obtained as follow

$$\delta u_0 = \frac{\partial N_{xx}}{\partial x} + \frac{\partial N_{xy}}{\partial y} = I_0\ddot{u}_0 - I_1\frac{\partial\ddot{w}_b}{\partial x} - J_1\frac{\partial\ddot{w}_s}{\partial x}$$
$$\delta v_0 = \frac{\partial N_{xy}}{\partial x} + \frac{\partial N_{yy}}{\partial y} = I_0\ddot{v}_0 - I_1\frac{\partial\ddot{w}_b}{\partial y} - J_1\frac{\partial\ddot{w}_s}{\partial y}$$
$$\delta w_b = \frac{\partial^2 M^b_{xx}}{\partial x^2} + 2\frac{\partial^2 M^b_{xy}}{\partial x\partial y} + \frac{\partial M^b_{yy}}{\partial y^2} - f_e$$
$$= I_0\left(\ddot{w}_b + \ddot{w}_s\right) + I_1\left(\frac{\partial\ddot{u}_0}{\partial x} + \frac{\partial\ddot{v}_0}{\partial y}\right) - I_2\nabla^2\ddot{w}_b - J_2\nabla^2\ddot{w}_s \tag{17}$$
$$\delta w_s = \frac{\partial^2 M^s_{xx}}{\partial x^2} + 2\frac{\partial^2 M^s_{xy}}{\partial x\partial y} + \frac{\partial M^s_{yy}}{\partial y^2} + \frac{\partial Q_x}{\partial x} + \frac{\partial Q_y}{\partial y} - f_e$$
$$= I_0\left(\ddot{w}_b + \ddot{w}_s\right) + J_1\left(\frac{\partial\ddot{u}_0}{\partial x} + \frac{\partial\ddot{v}_0}{\partial y}\right) - J_2\nabla^2\ddot{w}_b - K_2\nabla^2\ddot{w}_s,$$

The stress resultants N, M^b, M^s *and* Q of FG sandwich plate can be expressed as function of deformation by using Eq. (3) in Eq. (12) as

$$\begin{Bmatrix} N \\ M^b \\ M^s \end{Bmatrix} = \begin{bmatrix} A & B & B^s \\ B & D & D^s \\ B^s & D^s & H^s \end{bmatrix}\begin{Bmatrix} \varepsilon \\ k^b \\ k^s \end{Bmatrix}, \quad Q = A^s\gamma^0 \tag{18}$$

where

$$N = \{N_x, N_y, N_{xy}\}^t, \quad M^b = \{M^b_x, M^b_y, M^b_{xy}\}^t, \quad M^s = \{M^s_x, M^s_y, M^s_{xy}\}^t \tag{19a}$$

$$\varepsilon = \{\varepsilon^0_x, \varepsilon^0_y, \gamma^0_{xy}\}^t, \quad k^b = \{k^b_x, k^b_y, k^b_{xy}\}^t, \quad k^s = \{k^s_x, k^s_y, k^s_{xy}\}^t \tag{19b}$$

$$A = \begin{bmatrix} A_{11} & A_{12} & 0 \\ A_{12} & A_{22} & 0 \\ 0 & 0 & A_{66} \end{bmatrix}, \quad B = \begin{bmatrix} B_{11} & B_{12} & 0 \\ B_{12} & B_{22} & 0 \\ 0 & 0 & B_{66} \end{bmatrix}, \quad D = \begin{bmatrix} D_{11} & D_{12} & 0 \\ D_{12} & D_{22} & 0 \\ 0 & 0 & D_{66} \end{bmatrix} \tag{19c}$$

$$B^s = \begin{bmatrix} B^s_{11} & B^s_{12} & 0 \\ B^s_{12} & B^s_{22} & 0 \\ 0 & 0 & B^s_{66} \end{bmatrix}, \quad D^s = \begin{bmatrix} D^s_{11} & D^s_{12} & 0 \\ D^s_{12} & D^s_{22} & 0 \\ 0 & 0 & D^s_{66} \end{bmatrix}, \quad H^s = \begin{bmatrix} H^s_{11} & H^s_{12} & 0 \\ H^s_{12} & H^s_{22} & 0 \\ 0 & 0 & H^s_{66} \end{bmatrix} \tag{19d}$$

$$Q = \{Q_{yz}, Q_{xz}\}^t, \quad \gamma^0 = \{\gamma^0_{yz}, \gamma^0_{xz}\}^t, \quad A^s = \begin{bmatrix} A^s_{44} & 0 \\ 0 & A^s_{55} \end{bmatrix} \tag{19e}$$

where A_{ij}, B_{ij}, etc., are the plate stiffness, defined by

$$\begin{Bmatrix} A_{11} & B_{11} & D_{11} & B^s_{11} & D^s_{11} & H^s_{11} \\ A_{12} & B_{12} & D_{12} & B^s_{12} & D^s_{12} & H^s_{12} \\ A_{66} & B_{66} & D_{66} & B^s_{66} & D^s_{66} & H^s_{66} \end{Bmatrix} = \sum_{n=1}^{3}\int_{h_{n-1}}^{h_n} Q^{(n)}_{11}\left(1, z, z^2, f(z), z\,f(z), f^2(z)\right)\begin{Bmatrix} 1 \\ \nu^{(n)} \\ \frac{1-\nu^{(n)}}{2} \end{Bmatrix} dz \tag{20a}$$

and

$$\left(A_{22}, B_{22}, D_{22}, B^s_{22}, D^s_{22}, H^s_{22}\right) = \left(A_{11}, B_{11}, D_{11}, B^s_{11}, D^s_{11}, H^s_{11}\right), \quad Q^{(n)}_{11} = \frac{E(z)}{1-\nu^2} \tag{20b}$$

$$A^s_{44} = A^s_{55} = \sum_{n=1}^{3}\int_{h_{n-1}}^{h_n} \frac{E(z)}{2(1+\nu)}[g(z)]^2 dz, \tag{20c}$$

By replacing the Eq. (7) and (18) into equation (17), the equations of motion can be expressed in terms of displacements (u_0, v_0, w_b and w_b) as follow

$$
\begin{aligned}
&A_{11}\frac{\partial^2 u_0}{\partial x^2}+A_{66}\frac{\partial^2 u_0}{\partial y^2}+(A_{12}+A_{66})\frac{\partial^2 v_0}{\partial x\partial y}-B_{11}\frac{\partial^3 w_b}{\partial x^3}-(B_{12}+2B_{66})\frac{\partial^3 w_b}{\partial x\partial y^2}\\
&-B_{11}^s\frac{\partial^3 w_s}{\partial x^3}-(B_{12}^s+2B_{66}^s)\frac{\partial^3 w_s}{\partial x\partial y^2}=I_0\ddot{u}_0-I_1\frac{\partial \ddot{w}_b}{\partial x}-J_1\frac{\partial \ddot{w}_s}{\partial x}\\
&A_{22}\frac{\partial^2 v_0}{\partial y^2}+A_{66}\frac{\partial^2 v_0}{\partial x^2}+(A_{12}+A_{66})\frac{\partial^2 u_0}{\partial x\partial y}-B_{22}\frac{\partial^3 w_b}{\partial y^3}-(B_{12}+2B_{66})\frac{\partial^3 w_b}{\partial x^2\partial y}\\
&-B_{22}^s\frac{\partial^3 w_s}{\partial y^3}-(B_{12}^s+2B_{66}^s)\frac{\partial^3 w_s}{\partial x^2\partial y}=I_0\ddot{v}_0-I_1\frac{\partial \ddot{w}_b}{\partial y}-J_1\frac{\partial \ddot{w}_s}{\partial y}\\
&B_{11}\frac{\partial^3 u_0}{\partial x^3}+(B_{12}+2B_{66})\frac{\partial^3 u_0}{\partial x\partial y^2}+(B_{12}+2B_{66})\frac{\partial^3 v_0}{\partial x^2\partial y}+B_{22}\frac{\partial^3 v_0}{\partial y^3}\\
&-D_{11}\frac{\partial^4 w_b}{\partial x^4}-D_{22}\frac{\partial^4 w_b}{\partial y^4}-2(D_{12}+2D_{66})\frac{\partial^4 w_b}{\partial x^2\partial y^2}-D_{11}^s\frac{\partial^4 w_s}{\partial x^4}-D_{22}^s\frac{\partial^4 w_s}{\partial y^4}\\
&-2(D_{12}^s+2D_{66}^s)\frac{\partial^4 w_s}{\partial x^2\partial y^2}-f_e=I_0(\ddot{w}_b+\ddot{w}_s)+I_1\left(\frac{\partial \ddot{u}_0}{\partial x}+\frac{\partial \ddot{v}_0}{\partial y}\right)\\
&-I_2\nabla^2\ddot{w}_b-J_2\nabla^2\ddot{w}_s\\
&B_{11}^s\frac{\partial^3 u_0}{\partial x^3}+(B_{12}^s+2B_{66}^s)\frac{\partial^3 u_0}{\partial x\partial y^2}+(B_{12}^s+2B_{66}^s)\frac{\partial^3 v_0}{\partial x^2\partial y}+B_{22}^s\frac{\partial^3 v_0}{\partial y^3}-D_{11}^s\frac{\partial^4 w_b}{\partial x^4}\\
&-D_{22}^s\frac{\partial^4 w_b}{\partial y^4}-2(D_{12}^s+2D_{66}^s)\frac{\partial^4 w_b}{\partial x^2\partial y^2}+A_{55}^s\frac{\partial^2 w_s}{\partial x^2}+A_{44}^s\frac{\partial^2 w_s}{\partial y^2}-H_{11}^s\frac{\partial^4 w_s}{\partial x^4}\\
&-2(H_{12}^s+2H_{66}^s)\frac{\partial^4 w_s}{\partial x^2\partial y^2}-H_{22}^s\frac{\partial^4 w_s}{\partial y^4}=I_0(\ddot{w}_b+\ddot{w}_s)+J_1\left(\frac{\partial \ddot{u}_0}{\partial x}+\frac{\partial \ddot{v}_0}{\partial y}\right)\\
&-J_2\nabla^2\ddot{w}_b-K_2\nabla^2\ddot{w}_s
\end{aligned}
\tag{21}
$$

where the operator ∇^2 is given by

$$\nabla^2=\frac{\partial^2}{\partial x^2}+\frac{\partial^2}{\partial y^2} \tag{22}$$

3. Analytical solutions

In this investigation three boundary conditions are considered. The exact analytical solution of equations of motion (Eq. 21) for clamped (C) and simply supported (S) edges of FG-sandwich plate is presented. These boundary conditions of FG-sandwich plate are defined as:

Clamped (C)

$$u_0=v_0=w_b=\frac{\partial w_b}{\partial x}=\frac{\partial w_b}{\partial y}=w_s=\frac{\partial w_s}{\partial x}=\frac{\partial w_s}{\partial y}=0 \;\; at\;\; x=0,a;\;\; y=0,b. \tag{23}$$

Simply supported (S)

$$
\begin{aligned}
&v_0=w_b=\frac{\partial w_b}{\partial y}=w_s=\frac{\partial w_s}{\partial y}=0 \;\; at\;\; x=0,a.\\
&u_0=w_b=\frac{\partial w_b}{\partial x}=w_s=\frac{\partial w_s}{\partial x}=0 \;\; at\;\; y=0,b.
\end{aligned}
\tag{24}
$$

To satisfying the boundary conditions of Eqs. (23) and (24). The displacement components are given in the derivatives form as

$$
\begin{Bmatrix} u_0\\ v_0\\ w_b\\ w_s\end{Bmatrix}=\sum_{m=1}^{\infty}\sum_{n=1}^{\infty}\begin{Bmatrix} U_{mn}\dfrac{\partial X_m(x)}{\partial x}Y_n(y)e^{i\omega t}\\ V_{mn}X_m(x)\dfrac{\partial Y_n(y)}{\partial y}e^{i\omega t}\\ W_{bmn}X_m(x)Y_n(y)e^{i\omega t}\\ W_{smn}X_m(x)Y_n(y)e^{i\omega t}\end{Bmatrix}
\tag{25}
$$

Where the terms U_{mn}, V_{mn}, W_{bmn} and W_{smn} are coefficients $X_m(x)$ and $Y_n(y)$ are functions given in Table 1. ω Is the frequency with $i=\sqrt{-1}$.

The solution of the free vibrational analysis of FG-sandwich plate are obtained by substituting the analytical solution of Eq. (25) into the equations of motion of Eq. (21). the solution is in the matrix form as

$$
\left(\begin{bmatrix} S_{11} & S_{12} & S_{13} & S_{14}\\ S_{21} & S_{22} & S_{23} & S_{24}\\ S_{31} & S_{32} & S_{33} & S_{34}\\ S_{41} & S_{42} & S_{43} & S_{44}\end{bmatrix}-\omega^2\begin{bmatrix} M_{11} & 0 & M_{13} & M_{14}\\ 0 & M_{22} & M_{23} & M_{24}\\ M_{13} & M_{23} & M_{33} & M_{34}\\ M_{14} & M_{24} & M_{34} & M_{44}\end{bmatrix}\right)\begin{Bmatrix} U_{mn}\\ V_{mn}\\ W_{bmn}\\ W_{smn}\end{Bmatrix}=\begin{Bmatrix}0\\0\\0\\0\end{Bmatrix}
\tag{26}
$$

in which

$$
\begin{aligned}
&S_{11}=A_{11}\psi_{12}+A_{66}\psi_8\\
&S_{12}=(A_{12}+A_{66})\psi_8\\
&S_{13}=-B_{11}(\psi_8+\psi_{12})+2B_{66}\psi_8\\
&S_{14}=-(B_{12}^s+2B_{66}^s)\psi_8-B_{11}^s\psi_{12}\\
&S_{21}=(A_{12}+A_{66})\psi_{10}\\
&S_{22}=A_{22}\psi_4+A_{66}\psi_{10}\\
&S_{23}=-B_{22}\psi_4-(B_{12}+2B_{66})\psi_{10}\\
&S_{24}=-(B_{12}^s+2B_{66}^s)\psi_{10}-B_{22}^s\psi_4\\
&S_{31}=-B_{11}(e_{13}+e_{11})\\
&S_{32}=-B_{11}(e_{11}+e_5)\\
&S_{33}=D_{11}(e_{13}+e_5+2e_{11})+(\bar{N}_{xx}-k_{sx})e_9\\
&\qquad\qquad+(\bar{N}_{yy}-k_{sy})e_3+k_w e_1+2\bar{N}_{xy}e_7\\
&S_{34}=-D_{11}^s\left[(k_1+k_2\nu)e_{13}+2\bar{\nu}(k_1A'+k_2B')e_{14}+(k_1\nu+k_2)e_{11}\right]\\
&S_{41}=B_{11}^s\left[(k_1+k_2\nu)e_{15}+\bar{\nu}(k_1A'+k_2B')e_{16}\right]\\
&S_{42}=B_{11}^s\left[(k_1\nu+k_2)e_{17}+\bar{\nu}(k_1A'+k_2B')e_{16}\right]\\
&S_{43}=-D_{11}^s\left[(k_1+k_2\nu)e_{15}+2\bar{\nu}(k_1A'+k_2B')e_{16}+(k_1\nu+k_2)e_{17}\right]\\
&S_{44}=H_{11}^s(k_1^2+2\nu k_1k_2+k_2^2)e_{15}+\bar{\nu}H_{11}^s(k_1A'+k_2B')^2e_{18}\\
&\qquad\qquad-A_{55}^s\left[(k_1A')^2e_{19}+(k_2B')^2e_{16}\right]
\end{aligned}
\tag{27}
$$

and

$$
\begin{aligned}
&M_{11}=-I_0\psi_6 \qquad M_{12}=0\\
&M_{13}=I_1\psi_6 \qquad M_{14}=J_1\psi_6\\
&M_{22}=-I_0\psi_2 \qquad M_{23}=I_1\psi_2\\
&M_{24}=J_1\psi_2 \qquad M_{31}=I_1\psi_9\\
&M_{32}=-I_1\psi_3 \qquad M_{41}=-J_1\psi_9\\
&M_{33}=I_0\psi_1-I_2(\psi_9+\psi_3)\\
&M_{34}=M_{43}=-I_0\psi_1+J_2(\psi_3+\psi_9)\\
&M_{42}=-J_1\psi_3\\
&M_{44}=-I_0\psi_1+K_2(\psi 3+\psi_9)
\end{aligned}
\tag{28}
$$

with

$$
\begin{aligned}
&(\psi_1,\psi_3,\psi_5)=\int_0^b\int_0^a\left(X_mY_n,\; X_mY_n'',\; X_mY_n''''\right)X_mY_n\,dxdy\\
&(\psi_2,\psi_4,\psi_{10})=\int_0^b\int_0^a\left(X_mY_n', X_mY_n''', X_m''Y_n'\right)X_mY_n'\,dxdy\\
&(\psi_6,\psi_8,\psi_{12})=\int_0^b\int_0^a\left(X_m'Y_n, X_m'Y_n'', X_m'''Y_n\right)X_m'Y_n\,dxdy\\
&(\psi_7,\psi_9,\psi_{11},\psi_{13})=\int_0^b\int_0^a\left(X_m'Y_n', X_m''Y_n, X_m''Y_n'', X_m''''Y_n\right)X_mY_n\,dxdy
\end{aligned}
\tag{29}
$$

Table 1 The admissible functions $X_m(x)$ and $Y_n(y)$ of SSSS, CCCC and CSCS FG-sandwich plate.

Boundary conditions			The functions $X_m(x)$ and $Y_n(y)$	
SSSS	$X_m(0)=X''_m(0)=0$ $X_m(a)=X''_m(a)=0$	$Y_n(0)=Y''_n(0)=0$ $Y_n(b)=Y''_n(b)=0$	$sin(\lambda x)$	$sin(\mu y)$
CCCC	$X_m(0)=X'_m(0)=0$ $X_m(a)=X'_m(a)=0$	$Y_n(0)=Y'_n(0)=0$ $Y_n(b)=Y'_n(b)=0$	$sin^2(\lambda x)$	$sin^2(\mu y)$
CSCS	$X_m(0)=X'_m(0)=0$ $X_m(a)=X''_m(a)=0$	$Y_n(0)=Y'_n(0)=0$ $Y_n(b)=Y''_n(b)=0$	$\sin(\lambda x)[\cos(\lambda x)-1]$	$\sin(\mu y)[\cos(\mu y)-1]$

– ( )' denotes the derivative with respect to the corresponding coordinates.

In the current model, the non-trivial solution is obtained when "$\det([S]-\omega^2[M])=0$".

4. Results and discussions

In the following section, Several example for dynamic analysis of FG-sandwich plates reposed on elastic foundation are presented to show the accuracy and efficiency of the present refined four variable unknown model. The material properties of the FGM are summarized in the Table 2.

In the presented examples, six kinds of sandwich plates are utilized (1-0-1, 1-1-1, 1-2-1, 1-3-1, 2-1-2 and 2-2-1). The upper and lower interfaces of core (h_1, h_2) vary according to the configuration of the plate as presented in the Table 3.

In the current work, all numerical results are presented in the dimensionless form as

Table 2 Material properties of Ceramic and Metal

Properties	Metal	Ceramic
	Al	Al_2O_3
E (GPa)	70	380
ν	0.3	0.3
ρ (kg/m^3)	2707	3800

Table 3 Various layer thickness ratio of sandwich plates

layer thickness ratio	h_0	h_1	h_2	h_3
1-0-1	-h/2	0	0	h/2
1-1-1	-h/2	-h/6	h/6	h/2
1-2-1	-h/2	-h/4	h/4	h/2
1-3-1	-h/2	-3h/10	3h/10	h/2
2-1-2	-h/2	-h/10	h/10	h/2
2-2-1	-h/2	-h/10	3h/10	h/2

$$\omega^* = \omega\frac{a^2}{h}, \qquad \hat{\omega} = \frac{\omega b^2}{\pi^2}\sqrt{\rho h/D}$$

$$K_w = \frac{k_w a^4}{D}, \qquad K_s = \frac{k_s a^2}{D}, \qquad D = \frac{E_c h^3}{12(1-\nu^2)}$$

4.1 Validation

Table 4 present comparisons of dimensionless fundamental frequency $\hat{\omega}$ of a clamped homogeneous square plate (p=0) reposed on only Winkler foundation $K_s = 0$ with $(h/b = 0.015,\ \nu = 0.15)$. The obtained results are compared with those given by Sobhy (2013) using various shear deformation plate theories. A good agreement is achieved between current results and those of Sobhy (2013).

Table 5 give the dimensionless natural frequencies ($\hat{\omega}$) of simply supported square isotropic plate reposed on Winkler-Pasternak elastic foundation (K_w = varied, $K_s = 10$) for various mode number (m, n) and geometry ratio (b/h). The computed results are compared with those published by Sobhy (2013). It can be seen from the table that the current are in good agreement with those obtained by as Sobhy (2013). It can be also observed that the dimensionless natural frequencies ($\hat{\omega}$) are in direct correlation relation with vibration mode number (m, n) and Winkler parameter K_w.

Table 6 shows the effects of elastic foundation stiffnesses (K_w , K_s) and a/h and layer thickness ratio on the free vibration $(\bar{\omega})$ of various types of simply supported FG-sandwich square plates with (*p = 1.5*).

Table 4 Comparison of dimensionless fundamental frequency ($\hat{\omega}$) of a clamped homogeneous square plate resting on Winkler's elastic foundation

K_w	Sobhy (2013)	Present
1390.2	5.3330	5.3332
2780.4	6.5349	6.5351

Table 5 Comparison of natural frequency (ω^*) of a simply supported homogeneous square plate resting on Pasternak's elastic foundations

m	n	b/h	K_w	Sobhy (2013)	Present
1	1	100	100	2.6551	2.6551
			500	3.3400	3.3400
		10	200	2.7842	2.7842
			1000	3.9806	3.9806
2	1	100	100	5.5718	5.5718
			500	5.9287	5.9287
		10	200	5.3051	5.3049
			1000	6.0085	6.0083
2	2	100	100	8.5405	8.5405
			500	8.7775	8.7775
		10	200	7.7311	7.7303
			1000	8.2237	8.2229

Table 6 Effects of elastic foundation parameters (K_w and K_s) and geometry ratio a/h on the dimensionless f requency $\bar{\omega}$ of various types of simply supported sandwich square plates

Scheme	Theory	$k_w=k_s=0$			$k_w=100, k_s=0$			$k_w=100, k_s=100$		
		$a/h=5$	10	20	$a/h=5$	10	20	$a/h=5$	10	20
1-0-1	FSDPT(*)	0,9547	1,0167	1,0347	1,4061	1,461	1,4775	4,7803	4,8851	4,9134
	TSDPT(*)	0,9647	1,0198	1,0356	1,4121	1,4631	1,4781	4,7807	4,8854	4,9135
	SSDPT(*)	0,9655	1,02	1,0356	1,4125	1,4633	1,4781	4,7808	4,8854	4,9135
	ESDPT(*)	0,9663	1,0203	1,0357	1,4131	1,4635	1,4782	4,7808	4,8854	4,9135
	HSDPT(*)	0,9643	1,0196	1,0355	1,4119	1,463	1,4781	4,7805	4,8854	4,9135
	Present	0,9600	1,0152	1,0310	1,4057	1,4566	1,4716	4,7600	4,8640	4,892
1-1-1	FSDPT(*)	1,0717	1,1367	1,1555	1,1563	1,5227	1,5401	4,6538	4,7513	4,7788
	TSDPT(*)	1,0807	1,1395	1,1563	1,4695	1,5247	1,5407	4,6537	4,7517	4,7789
	SSDPT(*)	1,0817	1,1396	1,1563	1,4697	1,5248	1,5407	4,6537	4,7517	4,7789
	ESDPT(*)	1,0815	1,1398	1,1563	1,47	1,5249	1,5407	4,6537	4,7517	4,779
	HSDPT(*)	1,0816	1,1398	1,1563	1,4703	1,5249	1,5407	4,6538	4,7518	4,779
	Present	1,0774	1,1363	1,1531	1,4652	1,5204	1,5364	4,6408	4,7386	4,7658
1-2-1	FSDPT(*)	1,0717	1,1367	1,1555	1,1563	1,5227	1,5401	4,6538	4,7513	4,7788
	TSDPT(*)	1,0807	1,1395	1,1563	1,4695	1,5247	1,5407	4,6537	4,7517	4,7789
	SSDPT(*)	1,0817	1,1396	1,1563	1,4697	1,5248	1,5407	4,6537	4,7517	4,7789
	ESDPT(*)	1,0815	1,1398	1,1563	1,47	1,5249	1,5407	4,6537	4,7517	4,779
	HSDPT(*)	1,0816	1,1398	1,1563	1,4703	1,5249	1,5407	4,6538	4,7518	4,779
	Present	1,0774	1,1363	1,1531	1,4652	1,5204	1,5364	4,6408	4,7386	4,7658
1-3-1	FSDPT(*)	1,2605	1,346	1,371	1,5912	1,6688	1,692	4,5914	4,6898	4,719
	TSDPT(*)	1,2666	1,348	1,3716	1,5956	1,6704	1,6924	4,5911	4,6901	4,7192
	SSDPT(*)	1,2663	1,3479	1,3716	1,5954	1,6703	1,6924	4,591	4,6901	4,7192
	ESDPT(*)	1,2662	1,3478	1,3715	1,5953	1,6703	1,6924	4,5909	4,69	4,7192
	HSDPT(*)	1,2753	1,3506	1,3723	1,6024	1,6724	1,693	4,5921	4,6907	4,7194
	Present	1,2648	1,3459	1,3694	1,5933	1,6678	1,6898	4,5836	4,6827	4,7118

(*) given from Ref. Sobhy (2013).

Table 7 Dimensionless fundamental frequency $\bar{\omega}$ of FG-sandwich square plates (a=b, a/h=10) with various boundary conditions

Boundary conditions	p	Method	Scheme				
			1-0-1	2-1-2	1-1-1	2-2-1	1-2-1
SSSS	0	HySDT(*)	0.2956	0.2956	0.2956	0.2956	0.2956
		Present	0,2960	0,2960	0,2960	0,2960	0,2960
	0.5	HySDT(*)	0.5227	0.4846	0.4560	0.4366	0.4172
		Present	0,5229	0.4849	0.4564	0,4370	0.4177
	1	HySDT(*)	0.7454	0.6593	0.5954	0.5537	0.5124
		Present	0.7452	0.6593	0.5956	0.5540	0.5129
	2	HySDT(*)	1.0839	0.9254	0.8009	0.7200	0.6427
		Present	1.0830	0.9249	0.8008	0.7202	0.6431
	5	HySDT(*)	1.4519	1.2678	1.0767	0.9367	0.8131
		Present	1.4492	1.2659	1.0758	0.9364	0.8132
	10	HySDT(*)	1.5519	1.4053	1.2070	1.0392	0.8998
		Present	1.5489	1.4026	1.2055	1.0387	0.8996
CSCS	0	HySDT(*)	0.1836	0.1836	0.1836	0.1836	0.1836
		Present	0.1875	0.1875	0.1875	0.1875	0.1875
	0.5	HySDT(*)	0.3205	0.2972	0.2799	0.2682	0.2565
		Present	0.3251	0.3016	0.2842	0.2726	0.2608
	1	HySDT(*)	0.4546	0.4020	0.3634	0.3384	0.3134
		Present	0,4595	0,4066	0,3678	0,3429	0,3179
	2	HySDT(*)	0.6886	0.5615	0.4863	0.4379	0.3913
		Present	0,6637	0,5659	0,4908	0,4426	0,3960
	5	HySDT(*)	0.8835	0.7670	0.6513	0.5676	0.4931
		Present	0,8891	0,7708	0,6554	0,5722	0,4977
	10	HySDT(*)	0.9492	0.8503	0.7294	0.6290	0.5448
		Present	0,9569	0,8538	0,7331	0,6336	0,5494
CCCC	0	HySDT(*)	0.1606	0.1606	0.1606	0.1606	0.1606
		Present	0,1595	0,1595	0,1595	0,1595	0,1595
	0.5	HySDT(*)	0.2777	0.2576	0.2427	0.2327	0.2226
		Present	0,2766	0,2566	0,2418	0,2320	0,2219
	1	HySDT(*)	0.3922	0.3468	0.3137	0.2924	0.2710
		Present	0,3908	0,3458	0,3129	0,2917	0,2705
	2	HySDT(*)	0.5666	0.4825	0.4182	0.3770	0.3371
		Present	0,5641	0,4809	0,4171	0,3763	0,3367
	5	HySDT(*)	0.7610	0.6577	0.5584	0.4873	0.4236
		Present	0,7557	0,6545	0,5566	0,4861	0,4229
	10	HySDT(*)	0.8208	0.7292	0.6249	0.5396	0.4676
		Present	0,8139	0,7249	0,6224	0,5381	0,4667

(*) given from Ref. Abdelaziz *et al.* (2017).

From the comparisons in the Table 6, a good agreement is observed between computed results and those obtained via first-order shear deformation plate theory (FSDPT), third-order shear deformation plate theory (TSDPT), exponential shear deformation plate theory (ESDPT), hyperbolic shear deformation plate theory (HSDPT) and sinusoidal shear deformation plate theory (SSDPT) developed by Sobhy (2013). It can be also noted that the increase in the values of the geometry ratio (a/h) and foundation parameters (K_w , K_s) lead to increase the values of the fundamental frequency ($\bar{\omega}$) . The biggest values of the

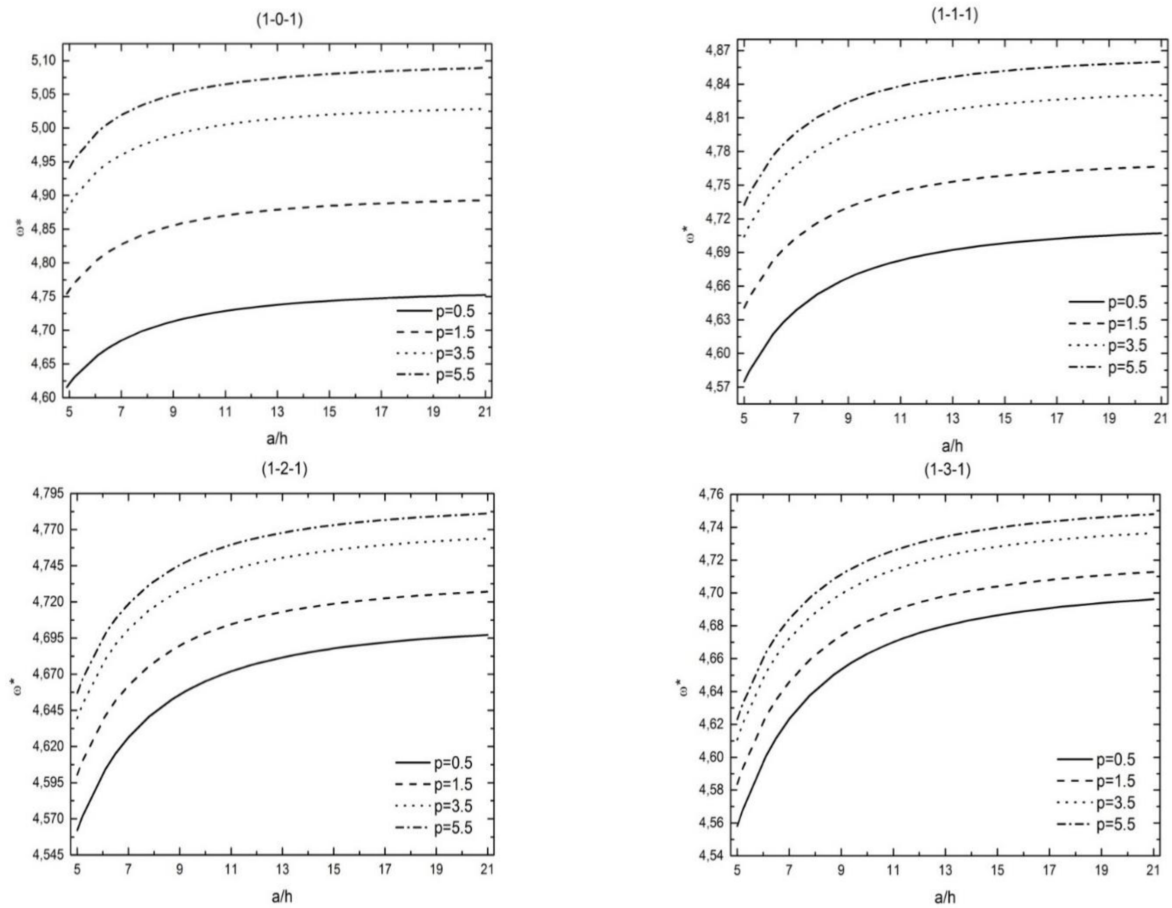

Fig. 2 Dimensionless fundamental frequency (ω^*) versuss the ratio *a/h* , layer thickness ratio and inhomogeneity parameter p of SSSS FGM sandwich square plates resting on elastic foundations $\left(K_w = K_s = 100\right)$

frequency ($\bar{\omega}$) are obtained for FG-sandwich plate with layer thickness ratio 1-3-1.

Table 7 gives dimensionless fundamental frequency $\bar{\omega}$ of SSSS, CCCC and CSCS FG-sandwich square plates with (a/h=10). The results are computed for ($p = 0$, 0.5, 1, 2, 5 and 10). A comparison is made between the current results and those of Abdelaziz *et al*. (2017). It can be confirmed again that the present model is in good agreement with those existing in the literature. It is clear in the table that the dimensionless fundamental frequency $\bar{\omega}$ increase with the increase of the face sheet material index (p). it can be also observed that the lower values of the $\bar{\omega}$ are obtained for clamped FG-sandwich plate.

4.2 Parametric study

In this part, parametric studies are presented to show the various parameters influencing the dynamic response of the FG-sandwich plate with various boundary conditions.

Fig. 2 display the variations of the frequencies (ω^*) versus the FG face sheet material index (p) and geometry ratio (a/h) for various layer thickness ratio of simply supported FG-sandwich square plates resting on elastic foundations $\left(K_w = K_s = 100\right)$.

From the obtained graphs, we can see that the frequency (ω^*) is in direct correlation relation with parameter (p) and side-to-thickness ratio a/h. It can also observed that the increase in the core thickness leads to reduce the differences between curves .

The effect of the inhomogeneity parameter *p* and Layer thickness ratio on fundamental frequency (ω^*) of simply supported and clamped FG-sandwich square plates with (a/h=10) are illustrated in the Fig. 3. From the plotted curves, it can be seen that the fundamental frequency (ω^*) is in inverse relation with parameters (p) because the FG faces sheet of the sandwich plate become metallic. The largest values of the fundamental frequency (ω^*) are obtained for FG-sandwich plate when the core thickness is twice that of the face sheet.

Fig. 4 plots the variation of the frequencies (ω^*) versus the geometry ratio (a/h) of SSSS, CCCC and CSCS EGM sandwich square plate with and without Winkler elastic foundation. From the obtained curves, It can be seen that the increase in the values of the ratio (a/h) leads to increase the eigen frequencies (ω^*) . We note also that the presence of the Winkler elastic foundation reduce the values of the

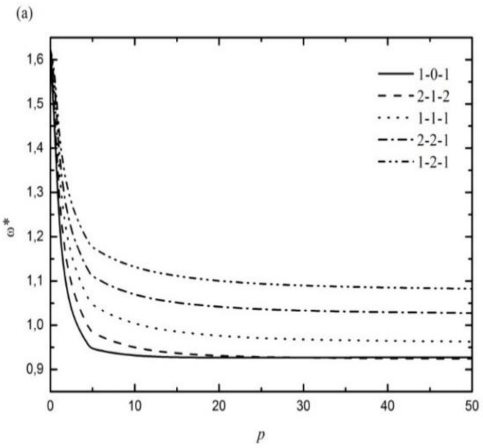

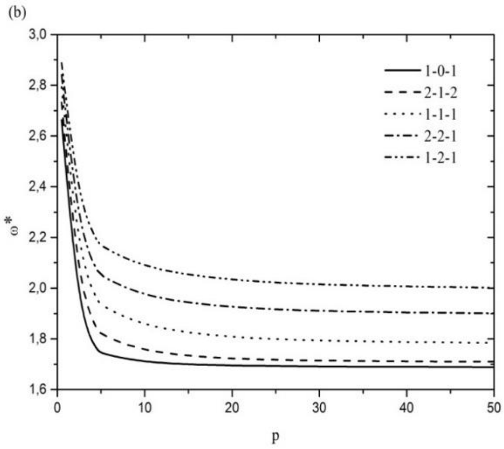

(a) clamped plate (*a/h*=10) (b) simply supported plate (*a/h*=10)

Fig. 3 Effect of the material index parameter (*p*) on non-dimensional frequency (ω^*) of square FG-sandwich plates

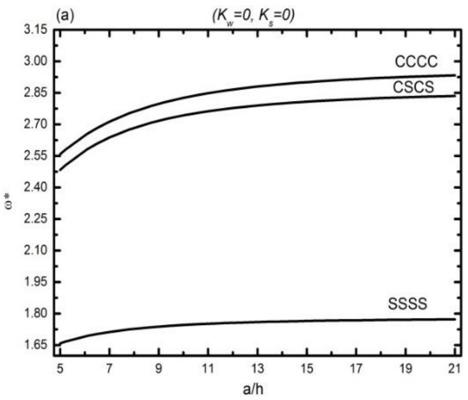

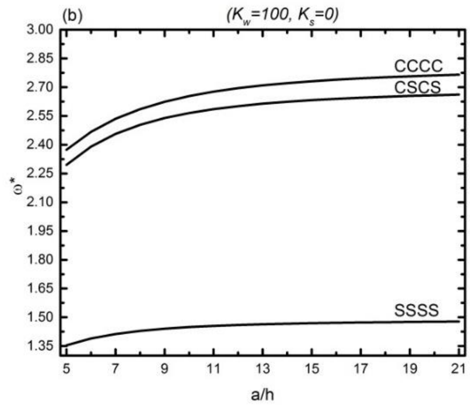

(a) clamped plate (*a/h*=10) (b) simply supported plate (*a/h*=10)

Fig. 4 Dimensionless frequency (ω^*) as function of geometry ratio *a/h* of the (1-2-1) CCCC, SSSS and CSCS EGM sandwich square plate with and without Winkler's elastic foundation (*p=0.5*)

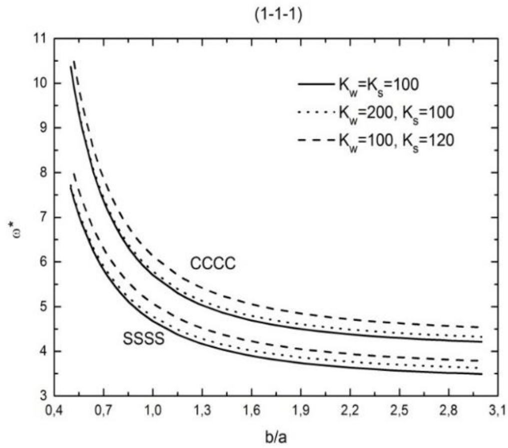

Fig. 5 variation of the frequencies (ω^*) versus ratio *b/a* of SSSS and CCCC sandwich plate for different values of Winkler-Pasternak parameters (K_w, K_s)

frequencies. It is clear also that the biggest values of (ω^*) are obtained for clamped plate.

The variation of the dimensionless frequencies (ω^*) versus the foundations parameters (K_w, K_s) and the dimension ratio *b/a* of clamped and simply supported plate with ($a/h = 10$, p=0.5) are plotted in the Fig. 5. It can be seen from the results that the dimensionless frequencies is in inverse relation with ratio b/a. the frequencies (ω^*) of the clamped plate are greater than that of simply supported plate. It can be concluded also that the presence of the Winkler-Pasternak elastic foundation has an important role on the values of the dimensionless frequencies (ω^*).

5. Conclusions

In this work, the dynamic response of two types of FG-sandwich plates with functionally graded faces sheets is investigated, using a four-variable refined plate model. The equations of motion are determined on the basis of the Hamilton's principle. The problem of various boundary conditions is solved analytically via Galerkin's approach. A comparison with the results of the literature is made to verify the accuracy and efficiency of current model. The effects of the material index, aspect, geometry and layer thickness ratio on dynamic response of the clamped and simply supported FG-sandwich plate are examined. Finally, an improvement of the present analytical model will be considered in the future work to consider other type of structures materials (Behera and Kumari 2018, Narwariya *et al*. 2018, Bensattalah *et al.* 2018, 2019a, b, Nikkhoo *et al*. 2019, López-Chavarría *et al.* 2019, Bakhshi and Taheri-Behrooz 2019, Singh and Kumari 2020, Ghannadpour and Mehrparvar 2020, Al-Maliki *et al.* 2020, Rachedi *et al.* 2020, Abed and Majeed 2020).

Acknowledgments

The first author would like to acknowledge the support provided by the Directorate General for Scientific Research and Technological Development (DGRSDT).

References

Abdelaziz H.H., Meziane M.A.A, Bousahla A.A., Tounsi A., Mahmoud S.R. and Alwabli A.S. (2017), "An efficient hyperbolic shear deformation theory for bending, buckling and free vibration of FGM sandwich plates with various boundary conditions", *Steel Compos. Struct.*, **25**(6), 693-704. http://dx.doi.org/10.12989/scs.2017.25.6.693.

Abdelmalek, A., Bouazza, M., Zidour, M. and Benseddiq, N. (2019), "Hygrothermal effects on the free vibration behavior of composite plate using nth-order shear deformation theory: a micromechanical approach", *Iran J. Sci. Technol. Trans. Mech. Eng*., **43**, 61-73. https://doi.org/10.1007/s40997-017-0140-y.

Abed, Z.A.K. and Majeed, W.I. (2020), "Effect of boundary conditions on harmonic response of laminated plates", *Compos. Mater. Eng.,* **2**(2), 125-140. DOI: 10.12989/cme.2020.2.2.125.

Akavci, S.S. (2016), "Mechanical behavior of functionally graded sandwich plates on elastic foundation", *Compos. Part B: Eng*., **96**, 136-152. doi:10.1016/j.compositesb.2016.04.035.

Al-Maliki, A.F.H., Ahmed, R.A., Moustafa, N.M. and Faleh, N.M. (2020), "Finite element based modeling and thermal dynamic analysis of functionally graded graphene reinforced beams", *Adv. Comput. Design,* **5**(2), 177-193. https://doi.org/10.12989/acd.2020.5.2.177.

Badriev, I.B., Makarov, M.V. and Paimushin, V.N. (2018), "Geometrically nonlinear problem of longitudinal and transverse bending of a sandwich plate with transversally soft core", *Lobachevskii Journal of Mathematics,* **39**(3), 448-457. doi:10.1134/s1995080218030046.

Bakhshi, N. and Taheri-Behrooz, F. (2019), "Length effect on the stress concentration factor of a perforated orthotropic composite plate under in-plane loading", *Compos. Mater. Eng*., **1**(1),71-90. https://doi.org/10.12989/cme.2019.1.1.071.

Behera, S. and Kumari, P. (2018), "Free vibration of Levy-type rectangular laminated plates using efficient zig-zag theory", *Adv. Comput. Design*, **3**(3), 213-232. https://doi.org/10.12989/acd.2017.2.3.165.

Bensattalah, T., Zidour, M. and Daouadji, T. H. (2019b), "A new nonlocal beam model for free vibration analysis of chiral single-walled carbon nanotubes", *Compos. Mater. Eng.*, **1**(1), 21-31. https://doi.org/10.12989/cme.2019.1.1.021.

Bensattalah, T., Zidour, M. and Hassaine Daouadji, T. (2018), "Analytical analysis for the forced vibration of CNT surrounding elastic medium including thermal effect using nonlocal Euler-Bernoulli theory", *Adv. Mater. Res*., **7**(3), 163-174. https://doi.org/10.12989/amr.2018.7.3.163.

Bensattalah, T., Zidour, M., Hassaine Daouadji, T. and Bouakaz, K. (2019a), "Theoretical analysis of chirality and scale effects on critical buckling load of zigzag triple walled carbon nanotubes under axial compression embedded in polymeric matrix", *Struct. Eng. Mech*., **70**(3), 269-277. https://doi.org/10.12989/sem.2019.70.3.269.

Chen, J., Zhang, W., Yao, M., Liu, J. and Sun, M. (2018), "Vibration reduction in truss core sandwich plate with internal nonlinear energy sink", *Compos. Struct*., **193**, 180-188. doi:10.1016/j.compstruct.2018.03.048.

Dinh Duc, N. and Hong Cong, P. (2016), "Nonlinear thermo-mechanical dynamic analysis and vibration of higher order shear deformable piezoelectric functionally graded material sandwich plates resting on elastic foundations", *J. Sandw. Struct. Mater*., **20**(2), 191-218. doi:10.1177/1099636216648488.

Do, T.V., Bui, T.Q., Yu, T.T., Pham, D.T. and Nguyen, C.T. (2017), "Role of material combination and new results of mechanical behavior for FG sandwich plates in thermal environment", *J. Comput. Sci*., **21**, 164-181. doi:10.1016/j.jocs.2017.06.015.

Dorduncu, M. (2020), "Stress analysis of sandwich plates with functionally graded cores using peridynamic differential operator and refined zigzag theory", *Thin-Wall. Struct*., **146**, 106468. doi:10.1016/j.tws.2019.106468.

Duc, N.D., Cong, P.H., Tuan, N.D., Tran, P., Anh, V.M. and Quang, V.D. (2015), "Nonlinear vibration and dynamic response of imperfect eccentrically stiffened shear deformable sandwich plate with functionally graded material in thermal environment", *J. Sandw. Struct. Mater*., **18**(4), 445–473. doi:10.1177/1099636215602142.

Ghannadpour, S.A.M. and Mehrparvar, M. (2020), "Modeling and evaluation of rectangular hole effect on nonlinear behavior of imperfect composite plates by an effective simulation technique", *Compos. Mater. Eng.,* **2**(1), 25-41. https://doi.org/10.12989/cme.2020.2.1.025.

Gholamzadeh babaki, M.H. and Shakouri, M. (2019), "Free and forced vibration of sandwich plates with electrorheological core and functionally graded face layers", *Mech. Based Des. Struct. Mach*., 1-18. doi:10.1080/15397734.2019.1698436.

Hosseini, M., Arani, A.G., Karamizadeh, M.R., Afshari, H. and Niknejad, S. (2019), "Aeroelastic analysis of cantilever non-symmetric FG sandwich plates under yawed supersonic flow", *Wind Struct*., **29**(6), 457-469. https://doi.org/10.12989/was.2019.29.6.457.

Iurlaro, L., Gherlone, M. and Di Sciuva, M. (2014), "Bending and free vibration analysis of functionally graded sandwich plates using the Refined Zigzag Theory", *J. Sandw. Struct. Mater.,* **16**(6), 669–699. doi:10.1177/1099636214548618.

Khorshidi, K. and Karimi, M. (2019), "Flutter analysis of sandwich plates with functionally graded face sheets in thermal environment", *Aerosp. Sci. Technol*., 105461. doi:10.1016/j.ast.2019.105461.

Kolahchi, R. (2017), "A comparative study on the bending, vibration and buckling of viscoelastic sandwich nano-plates based on different nonlocal theories using DC, HDQ and DQ methods", *Aerosp. Sci. Technol.*, **66**, 235-248. doi:10.1016/j.ast.2017.03.016.

Lal, A., Jagtap, K.R. and Singh, B.N. (2017), "Thermo-mechanically induced finite element based nonlinear static response of elastically supported functionally graded plate with random system properties", *Adv. Comput. Design*, **2**(3), 165-194. https://doi.org/10.12989/acd.2017.2.3.165.

Li, C., Shen, H.S. and Wang, H. (2020b), "Postbuckling behavior of sandwich plates with functionally graded auxetic 3D lattice core", *Compos. Struct.*, 111894. doi:10.1016/j.compstruct.2020.111894.

Li, C., Shen, H.S., Wang, H. and Yu, Z. (2020a), "Large amplitude vibration of sandwich plates with functionally graded auxetic 3D lattice core", *Int. J. Mech. Sci.,* 105472. doi:10.1016/j.ijmecsci.2020.105472.

Li, D., Deng, Z., Xiao, H., & Jin, P. (2018), "Bending analysis of sandwich plates with different face sheet materials and functionally graded soft core", *Thin-Walled Structures.,* **122**, 8–16. doi:10.1016/j.tws.2017.09.033.

Liu, H., Lv, Z. and Wu, H. (2019), "Nonlinear free vibration of geometrically imperfect functionally graded sandwich nanobeams based on nonlocal strain gradient theory", *Compos. Struct.*, doi:10.1016/j.compstruct.2019.01.090.

López-Chavarría, S., Luévanos-Rojas, A., Medina-Elizondo, M., Sandoval-Rivas, R. and Velázquez-Santillán, F. (2019), "Optimal design for the reinforced concrete circular isolated footings", *Adv. Comput. Design*, **4**(3), 273-294. https://doi.org/10.12989/acd.2019.4.3.273.

Mehar K., Panda S.K., Devarajan Y. and Choubey G. (2019), "Numerical buckling analysis of graded CNT-reinforced composite sandwich shell structure under thermal loading", *Compos. Struct.*, **216**, 406-414. https://doi.org/10.1016/j.compstruct.2019.03.002.

Mirzaalian, M., Aghadavoudi, F. and Moradi-Dastjerdi, R. (2019), "Bending Behavior of Sandwich Plates with Aggregated CNT-Reinforced Face Sheets", *J. Solid Mech.*, **11**(1), 26-38. doi: 10.22034/jsm.2019.664214.

Moita, J.S., Araújo, A.L., Correia, V.F., Mota Soares, C.M. and Herskovits, J. (2018), "Active-passive damping in functionally graded sandwich plate/shell structures", *Compos. Struct.*, doi:10.1016/j.compstruct.2018.01.089.

Moradi-Dastjerdi, R. and Behdinan, K. (2019), "Stability analysis of multifunctional smart sandwich plates with graphene nanocomposite and porous layers", *Int. J. Mech. Sci.*, 105283. doi:10.1016/j.ijmecsci.2019.105283.

Narwariya, M., Choudhury, A. and Sharma, A.K. (2018), "Harmonic analysis of moderately thick symmetric cross-ply laminated composite plate using FEM", *Adv. Comput. Design*, **3**(2), 113-132. https://doi.org/10.12989/acd.2018.3.2.113.

Nikkhoo, A., Asili, S., Sadigh, S., Hajirasouliha, I. and Karegar, H. (2019), "A low computational cost method for vibration analysis of rectangular plates subjected to moving sprung masses", *Adv. Comput. Design.,* **4**(3), 307-326. https://doi.org/10.12989/acd.2019.4.3.307.

Pagani, A., Valvano, S. and Carrera, E. (2016), "Analysis of laminated composites and sandwich structures by variable-kinematic MITC9 plate elements", *J. Sandw. Struct. Mater.*, **20**(1), 4-41. doi:10.1177/1099636216650988.

Pandey, S. and Pradyumna, S. (2018), "Analysis of functionally graded sandwich plates using a higher-order layerwise theory", *Composites Part B: Engineering.* doi:10.1016/j.compositesb.2018.08.121.

Rachedi, M.A., Benyoucef, S., Bouhadra, A., Bachir Bouiadjra, R., Sekkal, M. and Benachour, A. (2020), "Impact of the homogenization models on the thermoelastic response of FG plates on variable elastic foundation", *Geomech. Eng.*, **22**(1), 65-80. https://doi.org/10.12989/gae.2020.22.1.065.

Rekatsinas, C.S. and Saravanos, D.A. (2017), "A hermite spline layerwise time domain spectral finite element for guided wave prediction in laminated composite and sandwich plates", *J. Vib. Acoust.*, **139**(3), 031009. doi:10.1115/1.4035702.

Rezaiee-Pajand, M., Arabi, E. and Masoodi, A.R. (2019), "Nonlinear analysis of FG-sandwich plates and shells", *Aerosp. Sci. Technol.*, doi:10.1016/j.ast.2019.02.017.

Rezaiee-Pajand, M., Masoodi, A.R. and Mokhtari, M. (2018), "Static analysis of functionally graded non-prismatic sandwich beams", *Adv. Comput. Design.*, **3**(2), 165-190. https://doi.org/10.12989/acd.2018.165.

Safa, A., Hadji, L., Bourada, M. and Zouatnia, N. (2019), "Thermal vibration analysis of FGM beams using an efficient shear deformation beam theory", *Earthq. Struct.*, **17**(3), 329-336. https://doi.org/10.12989/eas.2019.17.3.329.

Sahouane, A., Hadji, L. and Bourada, M., (2019), "Numerical analysis for free vibration of functionally graded beams using an original HSDBT", *Earthq. Struct.*, **17**(1), 31-37. https://doi.org/10.12989/eas.2019.17.1.031.

Shokrieh, M.M. and Kondori, M.S, (2020), "Effects of adding graphene nanoparticles in decreasing of residual stresses of carbon/epoxy laminated composites", *Compos. Mater. Eng.*, **2**(1),53-64. https://doi.org/10.12989/cme.2020.2.1.053.

Singh, A. and Kumari, P. (2020), "Analytical free vibration solution for angle-ply piezolaminated plate under cylindrical bending: A piezo-elasticity approach", *Adv. Comput. Design.,* **5**(1), 55-89. https://doi.org/10.12989/acd.2020.5.1.055.

Sobhy, M. (2013), "Buckling and free vibration of exponentially graded sandwich plates resting on elastic foundations under various boundary conditions", *Compos. Struct.*, **99**, 76–87. http://dx.doi.org/10.1016/j.compstruct.2012.11.018.

Szekrényes, A. (2018), "The role of transverse stretching in the delamination fracture of softcore sandwich plates", *Appl. Math. Model.,* **63**, 611-632. doi:10.1016/j.apm.2018.07.014.

Tan, P., Nguyen-Thanh, N. and Zhou, K. (2017), "Extended isogeometric analysis based on Bézier extraction for an FGM plate by using the two-variable refined plate theory", *Theor. Appl. Fracture Mech.*, **89**, 127-138. doi:10.1016/j.tafmec.2017.02.002.

Tan, P., Nguyen-Thanh, N., Rabczuk, T. and Zhou, K. (2018), "Static, dynamic and buckling analyses of 3D FGM plates and shells via an isogeometric-meshfree coupling approach", *Compos. Struct.*, **198**, 35–50. doi:10.1016/j.compstruct.2018.05.012.

Thai, C.H., Nguyen-Xuan, H., Bordas, S.P.A., Nguyen-Thanh, N. and Rabczuk, T. (2015), "Isogeometric analysis of laminated composite plates using the higher-order shear deformation theory", *Mech. Adv. Mater. Struct.*, **22**(6), 451-469. doi:10.1080/15376494.2013.779050.

Tornabene, F. and Brischetto, S. (2018), "3D capability of refined GDQ models for the bending analysis of composite and sandwich plates, spherical and doubly-curved shells", *Thin-Wall. Struct.,* **129**, 94-124. doi:10.1016/j.tws.2018.03.021.

Tornabene, F., Fantuzzi, N. and Bacciocchi, M. (2017), "Foam core composite sandwich plates and shells with variable stiffness: Effect of the curvilinear fiber path on the modal response", *J. Sandw. Struct. Mater.,* 109963621769362. doi:10.1177/1099636217693623.

Tossapanon, P. and Wattanasakulpong, N. (2017), "Flexural vibration analysis of functionally graded sandwich plates resting on elastic foundation with arbitrary boundary conditions: Chebyshev collocation technique", *J. Sandw. Struct. Mater.*, 109963621773600. doi:10.1177/1099636217736003.

Yoosefian, A.R., Golmakani, M.E. and Sadeghian, M. (2019), "Nonlinear bending of functionally graded sandwich plates under mechanical and thermal load", *Communications in Nonlinear Science and Numerical Simulation.,*

105161. doi:10.1016/j.cnsns.2019.105161.
Zouatnia, N. and Hadji, L. (2019), “Static and free vibration behavior of functionally graded sandwich plates using a simple higher order shear deformation theory”, *Adv. Mater. Res.*, **8**(4), 313-335. https://doi.org/10.12989/amr.2019.8.4.313.

CC